Influence of Groove Parameters on Formation of Pear-shaped Bead Cracking in Narrow Gap Welding†

WU Yanming*, SIBAHARA Masakazu**, NAKAMURA Terumi*** and MURAKAWA Hidekazu****

Abstract

Narrow gap welding (NGW), which is effective in reducing heat input and achieving high productivity, is often employed in thick wall welding. However, for NGW, when the welding condition is not correctly selected, pear-shaped bead cracking will occur. The groove parameters have a significant influence on pear-shaped bead cracking. In this research, the effects of groove parameters on pear-shaped bead cracking and effective penetration depth are analyzed in detail by using FEM employing a temperature dependent interface element. Then, the welding condition is optimized for different groove parameters to achieve maximum effective penetration depth and maximum effective penetration depth per unit heat input, but without cracking.

KEY WORDS: (Narrow gap welding) (Pear-shaped bead cracking) (Interface element) (Groove parameter) (Effective penetration depth) (Heat distribution) (Optimization)

1. Introduction

Narrow gap welding (NGW) is one of the good choices for joining thick plates, because it has advantage in both cost saving and improved productivity. In addition, it can minimize the reduction of the toughness of the heat affected zone (HAZ) and the welding distortion due to the small heat input. However, the restraint is relatively high when a narrow gap is used. Welding cracks may occur if the welding conditions are not selected appropriately[1,2]. The cracking process can be simulated by using thermal-elastic-plastic FEM in which the temperature dependent interface element is adopted[3,4,5]. The simulation results are proved to agree with the experimental observation. The authors have previously discussed the influence of heat input distribution parameters on the formation of pear-shaped cracking[5]. In the present study, the influence of groove parameters on pear-shaped cracking in NGW are investigated in detail. Furthermore, the maximum effective penetation depth and effective penetraiton depth per unit heat input are obtained by using an optimization method, respectively.

2. Theoretical Model

Figure 1 shows the geometrical parameters of pear-shaped bead cracking, where P and W are penetration depth and width, respectively. W_T is the top width of the bead and P_E is the effective penetration depth of the bead. W_G and D_G are the groove width and depth of NGW, respectively. In order to clarify the process of the pear-shaped crack formation in narrow gap welding, a thermal-elastic-plastic FEM using temperature dependent

† Received on June 8, 2004
* Foreign Research Fellow, Associate Professor of Hefei University of Technology, China
** Lecturer, Kanazawa Institute of Technology
*** National Institute for Materials Science
**** Professor
Transactions of JWRI is published by Joining and Welding Research Institute of Osaka University, Ibaraki, Osaka 567-0047, Japan

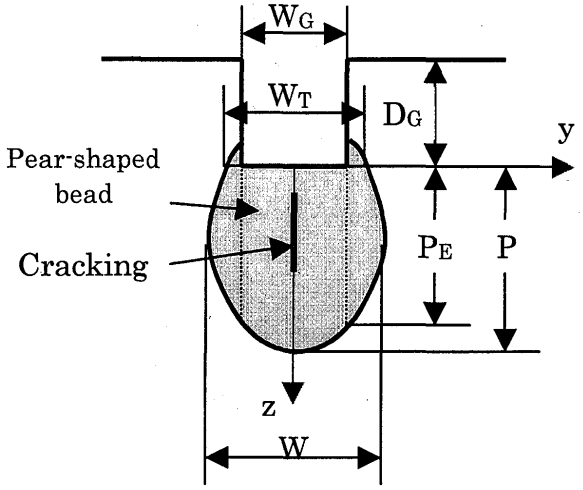

Fig. 1 Geometrical parameters of pear-shaped bead cracking.

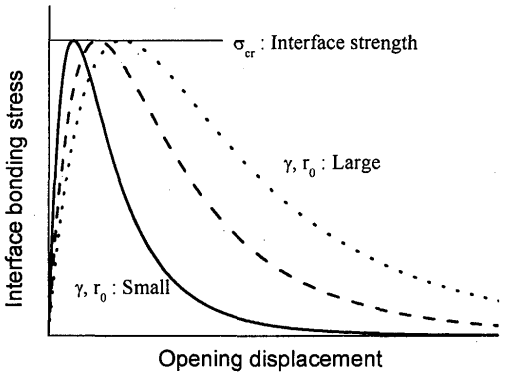

Fig. 2 Interface bonding stress-opening displacement curves of interface element.

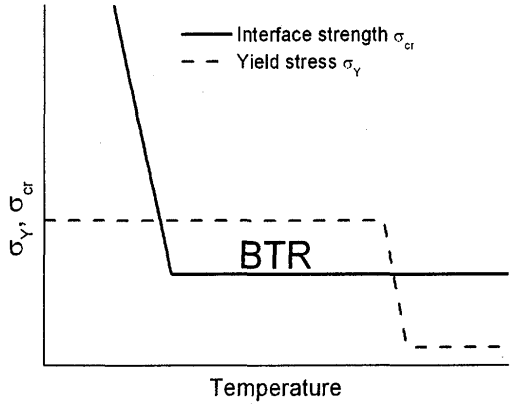

Fig. 3 Temperature dependent yield stress σ_y and interface strength σ_{cr}.

interface element is employed. Since the pear-shaped bead cracking occurs mostly along the centerline of the welding bead, the interface element is arranged along the center of the bead.

The mechanical behavior of the interface element is

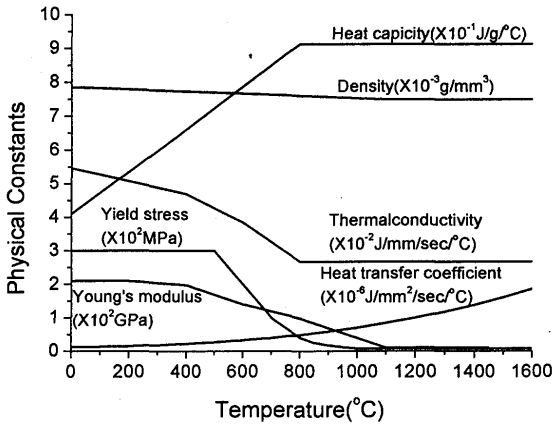

(a) Physical constants.

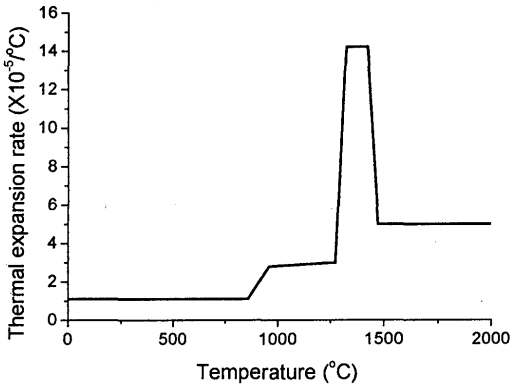

(b) Thermal expansion ratio.

Fig. 4 Temperature dependent physical constants.

governed by the interface potential per unit area of the crack surface, which is defined by the following equation.

$$\phi(\delta,T)=2\gamma(T)\left\{\left(\frac{r_0}{r_0+\delta}\right)^{2n}-2\left(\frac{r_0}{r_0+\delta}\right)^{n}\right\} \quad (1)$$

Where $\gamma(T)$ is the surface energy per unit area which is temperature dependent, while n and r_0 are constants independent of the temperature. The derivative of ϕ with respect to the crack opening δ gives the bonding stress σ, i.e.

$$\sigma=\frac{\partial\phi}{\partial\delta}=\frac{4n\gamma}{r_0}\left\{\left(\frac{r_0}{r_0+\delta}\right)^{n+1}-\left(\frac{r_0}{r_0+\delta}\right)^{2n+1}\right\} \quad (2)$$

The bonding strength per unit area reaches a maximum value under the following condition.

$$\frac{\delta}{r_0}=\left(\frac{2n+1}{n+1}\right)^{\frac{1}{n}}-1 \quad (3)$$

The maximum bonding strength σ_{cr} is given by,

$$\sigma_{cr}(T)=\frac{4\gamma(T)n}{r_0}\left\{\left(\frac{n+1}{2n+1}\right)^{\frac{n+1}{n}}-\left(\frac{n+1}{2n+1}\right)^{\frac{2n+1}{n}}\right\} \quad (4)$$

where σ_{cr} gives the critical strength at temperature T. Since σ_{cr} is proportional to $\gamma(T)$ as shown in Eq. (4), the temperature dependency of the surface energy γ is directly reflected in the critical strength σ_{cr}. The relation between the bonding stress σ and the opening displacement δ is presented in Fig. 2. As is shown in the figure, the parameter r_0 is a scale parameter. When r_0 is large, the opening displacement at the formation of the crack increases. By assuming that the surface energy is temperature dependent, the BTR (Solidification Brittleness Temperature Range) can be modeled as shown in Fig. 3.

The material considered here is SM490 and its temperature dependent physical constants used in the analysis are shown in Fig. 4(a). The thermal expansion ratio assumed to be also temperature dependent is shown in Fig. 4(b). The contraction during the solidification is considered through the thermal expansion ratio between 1300 °C and 1450 °C. The parameters included in the temperature dependent interface element are assumed as follows:

r_0=0.07 mm, n=6, BTR: 1350-1450°C

3. Heat Input Parameters for Narrow Gap Welding

In case of the arc welding, a normal (Gaussian) distribution which is given by the following equation is commonly used to model the heat source.

$$q(y,z)=Q\frac{1}{2\pi bc}e^{-\frac{(y-y_0)^2}{2b^2}}e^{-\frac{(z-z_0)^2}{2c^2}} \quad (5)$$

Where, Q is the heat input per unit length and it is related to the welding current I, voltage U, welding speed v and heat efficiency η, i.e.

$$Q=\eta UI/v \quad (6)$$

The parameters b and c are the characteristic width and depth which determine the heat distribution. For large b, the heat distribution is wide, and for large c, the heat distribution is deep.

4. Critical Penetration Depth for Crack Free Weld

It has been proved that there is a critical penetration depth P_C for a given heat input[5]. When the penetration depth is greater than the critical value, a pear-shaped cracking will occur for any combinations of heat input width b and depth c under the same heat input Q. On the other hand, when the penetration depth is less than the critical value, there is no cracking for any combinations of heat input width b and depth c under the same heat input Q.

In order to clarify the influence of the groove parameters on the crack formation, serial computations are performed. The groove width W_G is changed among the values of 3.2mm, 4.0mm, 5.0mm, 6.3mm, and the groove depth D_G is changed among the values of 2.0mm, 3.0mm, 4.0mm, 5.0mm, 10.0mm. The simulation results are summarized in **Fig. 5**. It is clearly seen that the critical penetration depth decreases along with an increase of heat input Q. In other words, when the heat input Q become larger, it is easier for cracking to occur. Figure 5(a) shows the critical penetration depth for different values of groove

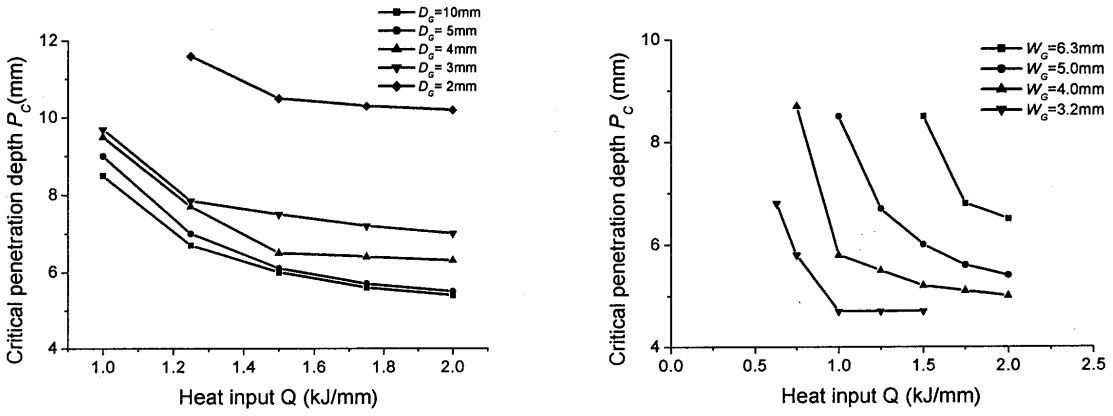

(a) Influence of groove depth.

(b) Influence of groove width.

Fig. 5 Relation between the critical penetration depth and groove parameters.

width W_G under the same groove depth D_G=10.0 mm. When groove width W_G is large, the critical penetration depth P_C become large for the same heat input Q, a pear-shaped crack seldom occurs. Figure 5(b) shows the critical penetration depth P_C for different values of groove depth D_G under the same groove width W_G =5.0 mm. When groove depth D_G is large, the critical penetration depth P_C become small for the same heat input Q and a pear-shaped crack easily occurs.

5. Effective Penetration Depth

As shown in Fig. 1, effective penetration depth P_E is the penetration depth for which the penetration width is larger than the groove width. When the top width of penetration W_T is less than the groove width W_G or a welding crack occurs, the weld fails. Therefore, in these cases, the effective penetration depth P_E is defined as 0. The influences of heat input parameters and groove parameters on the effective penetration depth P_E are investigated in the following.

5.1 Influence of heat input parameters

To examine the relation between the heat input parameters and the effective penetration depth, computed results of serial simulations are summarized in **Fig. 6**. In Fig. 6(a), the dashed lines show the penetration depth P, and the solid lines show the effective penetration depth P_E for different combinations of heat input width b and heat input depth c under the same heat input Q=1.25 kJ/mm, and the same groove parameters W_G=5.0 mm and D_G=3.0 mm. Fig. 6(b) shows the relation between effective penetration depth P_E and heat input Q for different heat input depth c. In general, the effective penetration depth P_E increases along with both an increase of heat input Q and heat input depth c, but the heat input width b has little influence on the values of effective penetration depth P_E. However, when heat input depth c is large, the effective penetration depth P_E may become 0 because of cracking or lack of fusion (i.e. the top width of penetration W_T is less than the groove width W_G). When the combinations of heat input depth c=4.0 mm, 5.0 mm, 6.0 mm and heat

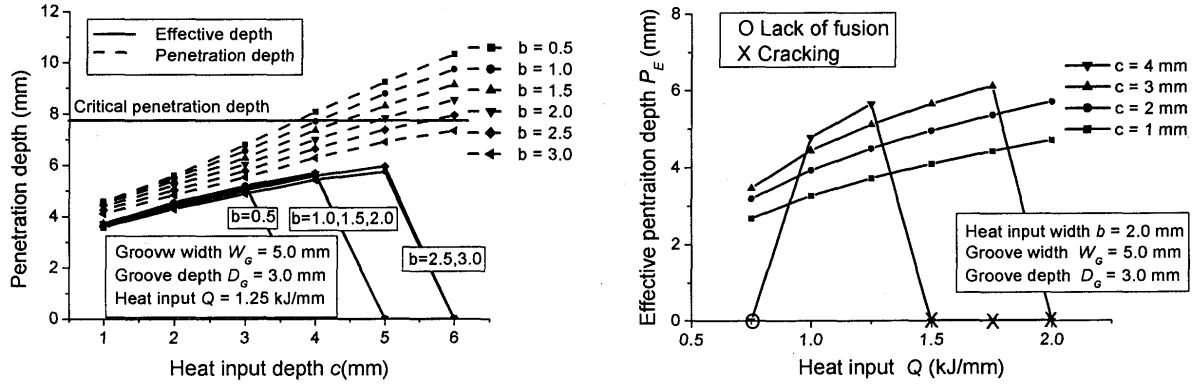

(a) Influence of heat distribution parameters. (b) Influence of heat input.

Fig. 6 Influence of heat input parameters on the effective penetration depth.

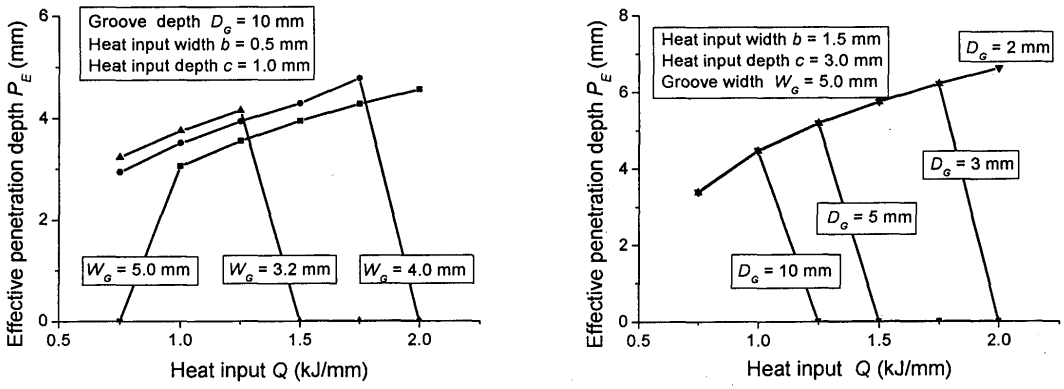

(a) Influence of groove width. (b) Influence of groove depth.

Fig. 7 Influence of groove parameters on the effective penetration depth.

input width b=0.5 mm are taken as examples, the penetration depth P is larger than the critical penetration depth P_C. Thus, the pear-shaped cracks will occur. The effective penetration P_E becomes 0 in those combinations as shown in Fig. 6(a). In case of the combination of heat input width b=3.0mm and depth c=6.0mm, the effective penetration depth P_E also becomes 0 because of the lack of fusion as shown in the same figure.

Then, the cases in which the heat input depth c=4.0 mm are selected for close examination as shown in Fig. 6(b). For the case of heat input Q=0.75 kJ/mm, because the heat input is not large enough, the top width of penetration W_T becomes less than the groove width W_G. Therefore, the effective penetration depth P_E becomes 0. When the heat input Q=1.50, 1.75, 2.00 kJ/mm, the heat input is too large so that pear-shaped cracks occur. Thus, the effective penetration depth P_E also becomes 0. Similarly, for the cases in which the heat input depth c=5.0 and 6.0 mm, all the effective penetration depths P_E become 0.

5.2 Influence of groove parameters

To clarify how the groove parameters influence the effective penetration depth, the computed results are summarized in **Fig. 7**. In general, the effective penetration depth increases with a decrease of groove width under the same heat input parameters, as shown in Fig. 7(a). For large groove widths, the top width of penetration may be less than the groove width when the heat input Q is small, e.g. the case in which heat input Q=0.75 kJ/mm, and groove width W_G=5.0 mm as shown in Fig. 7(a). On the other hand, for smaller groove widths, it is easier for cracking, in which the effective penetration become 0. Figure 7(b) shows the influence of groove depth on the effective penetration depth. If the factor of cracking is disregarded, the groove depth has no influence on the effective penetration depth. If the cracking is considered, cracks may occur when the groove depth is large. Therefore, the effective penetration depth becomes 0 for those cases.

Table 1 Maximum effective penetration depths for different groove widths under the same groove depth D_G =10.0mm.

W_G (mm)	Q (kJ/mm)	b (mm)	c (mm)	W_T (mm)	P_C (mm)	P (mm)	P_E (mm)
5.0	1.35	2.23	3.67	6.81	6.82	6.75	5.72
4.0	1.04	1.89	3.06	5.94	5.85	5.74	5.02
3.2	0.83	0.92	3.07	4.42	6.85	6.75	4.94
2.0	0.46	0.63	2.54	2.67	4.30	4.26	3.69
1.0	0.37	0.44	2.04	1.04	3.71	3.65	3.46

5.3 Optimization of effective penetration depth

Achieving the maximum effective penetration depth is one of the objectives of the NGW. An optimization method called the complex method[6] is employed to search the optimum values. The variables to be optimized are the heat input parameters, as shown in the following:

$$\{X\} = \{Q, b, c\} \tag{7}$$

The optimization problem can be written as,

$$\text{Maximize } F(X) = P_E \tag{8}$$

While seeking the optimum solution, the following constraints must be satisfied. (1) The constraint condition on the heat input parameters. (2) The weld must be crack free. (3) The top width of the penetration W_T must be greater than the groove width W_G to prevent lack of fusion.

The results of the optimization are summarized in **Table 1** and **Table 2** for different groove parameters, respectively. Table 1 shows that the maximum effective penetration depth P_E decreases along with a decrease of groove width. This can be explained by the fact that the critical penetration depth without cracking becomes small when the groove width becomes narrow. Similarly, Table 2 shows that the effective penetration increases along with a decease of groove depth, because cracking is less likely to occur when the groove is shallow.

6. Ratio of P_E/Q

The efficiency is another key factor of the welding. To achieve maximum effective penetration depth with minimum heat input is another objective of NGW. In this section, the ratio of P_E/Q is maximized based on the analysis of how the factors influence the ratio of P_E/Q.

6.1 Influence of heat input parameters

To clarify how the heat input parameters influence the ratio of P_E/Q, the results of serial simulations are summarized in **Fig. 8**. Similar to the influence on the effective penetration depth, the ratio P_E/Q increases along

Table 2 Maximum effective penetration depths for different groove widths under the same groove depth W_G=5.0mm.

D_G (mm)	Q (kJ/mm)	b (mm)	c (mm)	W_T (mm)	P_C (mm)	P (mm)	P_E (mm)
10.0	1.35	2.23	3.67	6.81	6.82	6.75	5.72
5.0	1.39	0.55	3.43	5.83	6.95	6.79	5.81
4.0	1.29	1.35	4.14	5.74	7.15	7.06	5.86
3.0	2.13	2.04	4.27	10.7	7.53	7.49	6.56
2.0	3.00	2.91	5.84	11.4	10.7	10.6	10.1

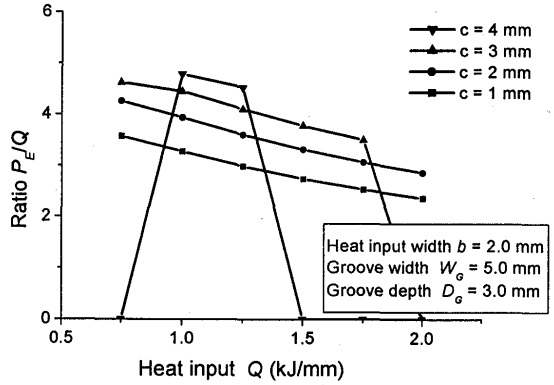

Fig. 8 Influence of heat input parameters on the ratio P_E/Q.

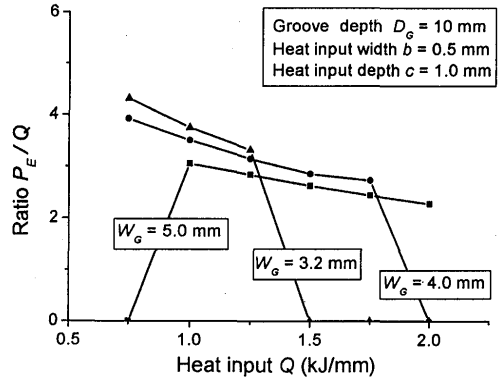

(a) Influence of groove width.

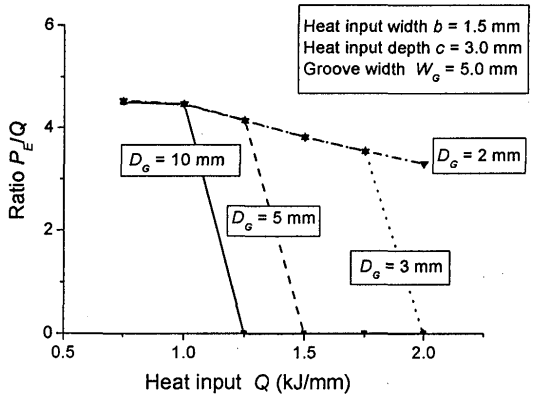

(b) Influence of groove depth.

Fig. 9 Influence of groove parameters on the ratio P_E/Q.

with an increase of heat input depth c. The heat input width b has very little influence on the ratio P_E/Q. However, the ratio P_E/Q decreases along with an increase of the heat input Q under the same heat distribution parameters and the same groove parameters.

6.2 Influence of groove parameters

To examine the influence of groove parameters on the ratio P_E/Q, the results of serial computations are summarized in **Fig. 9**. The influences of groove depth and groove width are shown in Figs. 9(a) and (b), respectively. Similar to the influence on the effective penetration depth, the ratio P_E/Q generally increases along with a decrease of groove width. The groove depth has no effect on the value of ratio P_E/Q, but the zone in which the ratio become 0 because of cracking is enlarged along with the increase of groove depth D_G.

6.3 Optimization of ratio P_E/Q

Similar to the optimization of the effective penetration depth, the same optimization method and the same variables are used to optimize the ratio P_E/Q. The objective function is changed as,

$$\text{Maximize } F(X) = P_E/Q \qquad (9)$$

The results of the optimization are summarized in **Table 3** and **Table 4**. As seen from Table 3, the ratio P_E/Q at the optimum condition increases with a decrease of groove width W_G under the same groove depth D_G. This comes from the fact that the aspect ratio of the effective penetration P_E/W_T at the optimum point increases with a decrease of the groove width W_G. This result may explain the reason why crack free welds can be achieved by the Laser Beam Welding and the Electron Beam Welding which are regarded as narrow gap welding with extremely small groove width W_G.

Table 4 shows that the groove depth contributes very little to the ratio P_E/Q under the same groove width. This

Table 3 Optimization of ratio P_E/Q for different groove widths under the same groove depth D_G =10.0mm

W_G (mm)	Q (kJ/mm)	b (mm)	c (mm)	W_T (mm)	P_E (mm)	P_E/W_T	P_E/Q (mm²/kJ)
5.0	1.12	2.22	4.67	5.40	5.45	1.01	4.87
4.0	0.89	1.12	4.65	4.03	5.18	1.29	5.80
3.2	0.69	1.09	4.28	3.28	4.74	1.45	6.86
2.0	0.43	0.42	3.06	2.10	3.61	1.72	8.43
1.0	0.36	0.63	3.15	1.03	3.57	3.59	9.89

Table 4 Optimization of ratio P_E/Q for different groove depths under the same groove depth W_G =5.0mm.

D_G (mm)	Q (kJ/mm)	b (mm)	c (mm)	W_T (mm)	P_E (mm)	P_E/W_T	P_E/Q (mm²/kJ)
10.0	1.12	2.22	4.67	5.4	5.45	1.01	4.87
5.0	1.17	1.90	4.99	5.27	5.71	1.08	4.88
4.0	1.13	2.14	5.31	5.01	5.54	1.10	4.90
3.0	1.20	2.14	5.23	5.36	5.88	1.09	4.90
2.0	1.54	2.00	7.29	5.30	7.65	1.44	4.97

can be explained by Fig. 9(b). The optimum results are located at the low heat input area, in which there is no crack for any condition.

6.4 Comparison of optimization of P_E and ratio P_E/Q

From Table 1 and Table 2, it is seen that the penetration depth P is close to the critical penetration P_C under the condition of maximum effective penetration depth. In other words, the maximum effective penetration is limited by pear-shaped cracking.

From Table 3 and Table 4, it is found that the top width of penetration W_T is close to the groove width under the condition of maximum effective penetration per unit of heat input. In other words, the maximum ratio of P_E/Q is mainly limited by lack of fusion.

7. Conclusions

By using a temperature dependent interface element, the influences of groove parameters on the crack formation and the effective penetration depth in narrow gap welding are closely examined. Based on the knowledge obtained from the present study, a method to optimize the heat input parameters to maximize the effective penetration depth without cracking is proposed. The conclusions can be summarized as follows.

(1) The groove parameters have a significant influence on crack formation in narrow gap welding. Cracking can happen when the groove is narrow and deep.

(2) The effective penetration depth becomes larger with an increase of heat input Q and heat input depth c. However, the heat input width b contributes very little to the effective penetration depth P_E.

(3) When the groove width becomes narrow, the maximum effective penetration depth P_E becomes smaller, but the maximum effective penetration depth per unit heat input P_E/Q become larger. For deeper groove welding, the maximum effective penetration depth becomes smaller, but the maximum ratio of P_E/Q changes very little for different groove depths under the same groove width.

(4) The maximum effective penetration depth P_E is limited by pear-shaped cracking, and the maximum effective penetration depth per unit heat of input P_E/Q is mainly limited by lack of fusion.

References

1) Mori Y and Masumoto I. "Consideration about the forming of the pear-shaped bead" JWS, Vol.48, No.12, pp1041-1047, 1979 (in Japanese).

2) Mori Y and Masumoto I. "Consideration about the forming of the pear-shaped bead crack" JWS, Vol.49, No.1, pp19-23, 1980 (in Japanese).

3) Shibahara M, Serizawa H, Murakawa H and Ueda Y. "Finite element analysis of hot cracking under welding using temperature dependent interface element" , the proceedings of the 11th international offshore and polar engineering conference, Vol.IV, pp.297-303, 2001.

4) Shibahara M, Itoh S, Liang W and Murakawa H. "Finite element simulation of pear-shaped bead cracking in narrow gap welding" . the proceedings of the 13th international offshore and polar engineering conference, Vol. IV , pp135-140,2003

5) Wu Yanming, Shibahara Masakazu, Nakamura Terumi and Murakawa Hidekazu. "Influence of heat input distribution parameters on formation of pear-shaped bead cracking in narrow gap welding". the proceedings of the 14th international offshore and polar engineering conference, Vol.IV, pp141-147,2004

6) Xu SL. "Useful Algorithms and Programmings for C Language", Tsinghua University Press, pp351-359,1994 (in Chinese)